

Symmetry breaking of a matter-wave soliton in a double-well potential formed by spatially confined spin-orbit coupling

Zhi-Jiang Ye, Yi-Xi Chen, Yi-Yin Zheng, Xiong-Wei Chen, Bin Liu*

School of Physics and Optoelectronic Engineering, Foshan University, Foshan 528000, China

We consider the symmetry breaking of a matter-wave soliton formed by spinor Bose-Einstein condensates (BECs) illuminated by a two-spot laser beam. This laser beam introduces spin-orbit (SO) coupling in the BECs such that the SO coupling produces an effect similar to a linear double-well potential (DWP). It is well known that symmetry breaking in a DWP is an important effect and has been discussed in many kinds of systems. However, it has not yet been discussed in a DWP formed by SO coupling. The objective of this work is to study the symmetry breaking of spinor BECs trapped by a DWP formed by SO coupling. We find that two kinds of symmetry breaking, displacement symmetry breaking and bimodal symmetry breaking, can be obtained in this model. The influence of the symmetry transition is systematically discussed by controlling the interaction strength of the BECs and the distance between the center of the two spots. Moreover, because SO coupling violates Galilean invariance, the influence of symmetry breaking in the moving system is also addressed in this paper.

PACS numbers: 03.75.Lm, 05.45.Yv

I. INTRODUCTION

Matter-wave solitons have become an interesting subject of research due to their potential applications in various fields, such as atomic interferometry, quantum information processing, and atomic lasers [1]. Experimental research on a self-trapping soliton in Bose-Einstein condensates (BECs) began with the creation of a dark soliton, followed by bright soliton and bright soliton trains [2–5]. Many studies have shown that a cold-atom BEC is an excellent system for studying solitons [6–10]. In particular, a stable bright soliton has already been shown to improve the performance of a Mach-Zehnder interferometer compared to regular BECs [11]. Thus, the creation of stable soliton has become a fascinating area of research.

Recently, the Gross-Pitaevskii equation (GPE) with the LHY correction term has been proven to be a good mechanism to generate stable quantum droplets [12–34], and the GP equation with long-range dipole-dipole interactions can also create stable matter-wave solitons in BECs [35–39]. With the help of spin-orbit (SO) coupling, absolutely stable (ground-state) and metastable matter-wave solitons in 2D and 3D free space have been reported [40–49]. Moreover, stable excited state solitons [50–54], gap solitons [55, 56], and solitons with novel vortices [57–62] have been reported to be created by SO coupling [63, 64], and similar configurations have also been realized in an optical system [65–69]. However, previous studies on 2D and 3D solitons in BECs with SO coupling tacitly assumed that the SO couplings were a homogeneous effect in the entire space. Recently, by using an external laser beam of a finite width, it was shown that one can implement spatially confined SO coupling, i.e., an SO coupling defect, in spinor BECs in 1D [70] and 2D [71] space. It is interesting to find that solitons are trapped and caught by the SO coupling with a spatially confined modulation. These results imply that spatially confined SO coupling can act as a trapping potential to trap the BECs in space.

If two of these beams, which form the SO coupling defect, are launched, an effective double-well potential (DWP) for the spinor BECs is created [see Fig.1]. It is well known that one of the fundamental aspects of the nonlinear dynamics in the DWP is spontaneous symmetry breaking (SSB), in which a symmetric state breaks its symmetry to a favorable asymmetric state. The concept of SSB in nonlinear systems was introduced by J. C. Eilbeck [72]. Its manifestations can be found in a variety of settings, including classical and quantum mechanics, dual-core optical waveguides and Bragg gratings, nonlinear discrete systems, nonlinear optics and other physical systems [72–75]. In particular, SSB effects were studied in detail in BECs [76–84]. Applications of this effect, such as the design of power-switch devices based on soliton light propagation in fibers, were proposed [85]. In BECs, the SSB of matter-wave solitons in a DWP has been considered in many configurations but not for matter-wave solitons in a DWP formed by spatially confined SO coupling. Hence, the mechanism of SSB in a DWP formed by SO coupling remains unclear.

*Electronic address: binliu@fosu.edu.cn

The objective of this work is to study the SSB of matter-wave solitons in a DWP formed by two spatially confined SO couplings in a 1D system. A sketch of the configuration of this system is shown in Fig. 1: spinor BECs with an attractive interaction are trapped in a horizontal cigar-shaped potential well, and two external laser illuminations, which form the spatially confined SO coupling, trap the BECs in their illumination area. We study the mechanism of SSB in such a DWP and find two types of symmetry breaking, displacement symmetry breaking and bimodal symmetry breaking. The mechanism of these two kinds of SSB are systematically discussed in this paper. Moreover, because SO coupling violates Galilean invariance, discussing the SSB in the moving system is a nontrivial issue, which is also discussed in detail in this paper. The rest of the paper is structured as follows. The model is introduced in Sec. II. Basic numerical results for the SSB of a matter-wave soliton in the quiescent and moving reference frames are reported in Sec. III. The paper is concluded in Sec. V.

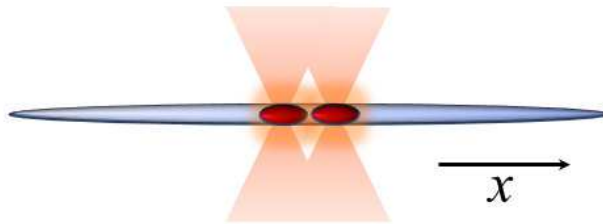


FIG. 1: (Color online) Sketch of the system. The spinor BECs are illuminated by a two-spot SO coupling beam, which traps the BECs in a new type of DWP.

II. THE MODEL

We consider binary BECs with a pseudo-spinor wave function $\Psi_+(x, t)$, $\Psi_-(x, t)$. The mean-field model of the system is based on the Lagrangian

$$\begin{aligned}
 L &= \int \mathcal{L} dx, \\
 \mathcal{L} &= -\frac{i}{2} \left(\Psi_+^* \frac{\partial \Psi_+}{\partial t} + \Psi_-^* \frac{\partial \Psi_-}{\partial t} - c.c. \right) + \frac{1}{2} \left(|\partial_x \Psi_+|^2 + |\partial_x \Psi_-|^2 \right) \\
 &\quad - \frac{g}{2} \left(|\Psi_+|^4 + |\Psi_-|^4 \right) - g\gamma |\Psi_+|^2 |\Psi_-|^2 + \frac{\lambda(x)}{2} \left\{ \left(\Psi_+^* \frac{\partial \Psi_-}{\partial x} - \Psi_-^* \frac{\partial \Psi_+}{\partial x} \right) + c.c. \right\}, \quad (1)
 \end{aligned}$$

where *c.c.* stands for a complex conjugate, γ is the relative strength of the cross-attraction, and the strength of the self-attraction is normalized to 1. g is the total nonlinear strength. The SO coupling of the Rashba type, which has a double-well structure, is

$$\lambda(x) = \lambda_0 \exp \left[-(x - x_0)^2 / D^2 \right] + \lambda_0 \exp \left[-(x + x_0)^2 / D^2 \right], \quad (2)$$

where $\lambda_0 \equiv 1$ is the normalized peak strength of the SO coupling, x_0 denotes the half distance between the two wells, and D is the width of the well, i.e., the width of the spots of the illumination.

The Gross-Pitaevskii equation (GPE) is derived from Lagrangian (1) using the Euler-Lagrange equations as follows:

$$\begin{aligned}
 i \frac{\partial \Psi_+}{\partial t} &= -\frac{1}{2} \frac{\partial^2 \Psi_+}{\partial x^2} - g \left(|\Psi_+|^2 + \gamma |\Psi_-|^2 \right) \Psi_+ + \lambda(x) \frac{\partial \Psi_-}{\partial x} + \frac{\lambda_x(x)}{2} \Psi_-, \\
 i \frac{\partial \Psi_-}{\partial t} &= -\frac{1}{2} \frac{\partial^2 \Psi_-}{\partial x^2} - g \left(|\Psi_-|^2 + \gamma |\Psi_+|^2 \right) \Psi_- - \lambda(x) \frac{\partial \Psi_+}{\partial x} - \frac{\lambda_x(x)}{2} \Psi_+. \quad (3)
 \end{aligned}$$

Stationary solutions to Eqs. (3) with a chemical potential μ are sought as

$$\Psi_{\pm}(x, t) = \phi_{\pm}(x) e^{-i\mu t}, \quad (4)$$

where the functions $\phi_{\pm}(x)$ satisfy the equations

$$\begin{aligned}\mu\phi_+ &= -\frac{1}{2}\frac{\partial^2\phi_+}{\partial x^2} - g\left(|\phi_+|^2 + \gamma|\phi_-|^2\right)\phi_+ + \lambda(x)\frac{\partial\phi_-}{\partial x} + \frac{\lambda_x(x)}{2}\phi_-, \\ \mu\phi_- &= -\frac{1}{2}\frac{\partial^2\phi_-}{\partial x^2} - g\left(|\phi_-|^2 + \gamma|\phi_+|^2\right)\phi_- - \lambda(x)\frac{\partial\phi_+}{\partial x} - \frac{\lambda_x(x)}{2}\phi_+, \end{aligned} \quad (5)$$

which can be derived from their own Lagrangian density:

$$\begin{aligned}\mathcal{L}_{stat} &= -\mu\left(|\phi_+|^2 + |\phi_-|^2\right) + \frac{1}{2}\left(|\partial_x\phi_+|^2 + |\partial_x\phi_-|^2\right) \\ &\quad - \frac{1}{2}g\left(|\phi_+|^4 + |\phi_-|^4\right) - \gamma|\phi_+|^2|\phi_-|^2 + \frac{\lambda(x)}{2}\left\{\left(\phi_+^*\frac{\partial\phi_-}{\partial x} - \phi_-^*\frac{\partial\phi_+}{\partial x}\right) + c.c.\right\} \end{aligned} \quad (6)$$

The total norm of ansatz (4) is

$$N = \int n(x)dx = \int \left(|\phi_+|^2 + |\phi_-|^2\right) dx \quad (7)$$

where $n(x) = |\phi_+(x)|^2 + |\phi_-(x)|^2$ is the total density pattern soliton. The solution of the matter-wave soliton of Eq. (5) is solved numerically by means of the imaginary-time-integration method [86, 87]. In addition, the stabilities are verified by direct simulations. To study the mechanism of SSB in such a DWP clearly, we will apply the normalized condition to the total norm of the soliton and fix the value of D in the numerical simulations. Hence, the free control parameters for the system are the nonlinear strength g , the strength of the cross-interaction γ , and the distance between the two wells, x_0 . Here, larger values of g and smaller values of x_0 correspond to a stronger attractive nonlinearity and coupling between the two wells, respectively.

III. SYMMETRIC AND ASYMMETRIC SOLUTIONS

A. Quiescent reference frame

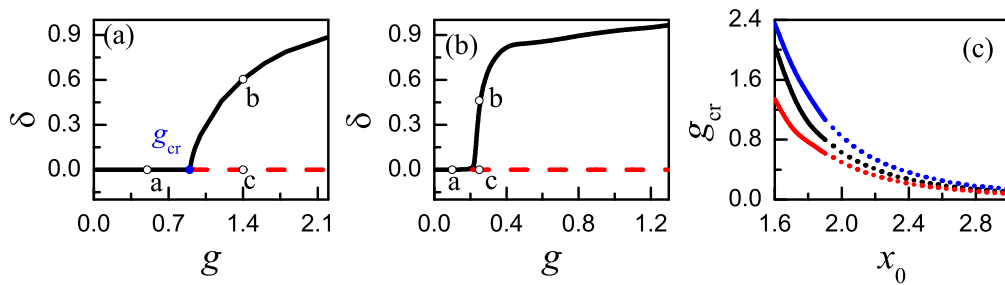


FIG. 2: (Color online) Bifurcation diagrams for the symmetric and asymmetric solutions, in the plane of (g, δ) , as found from the numerical solution of Eq. (5) at different values of x_0 . (a) $x_0 = 1.85$; (b) $x_0 = 2.5$. (c) The blue, black, and red curves show the displacement supercritical points for $\gamma = 0, 1$, and 2 , respectively. The blue, black, and red dashed curves show the bimodal supercritical points for $\gamma = 0, 1$, and 2 , respectively.

To identify the mechanism of the SSB precisely, we define the asymmetric character as follows:

$$\delta = \left| \frac{n_L^{\max} - n_R^{\max}}{n_L^{\max} + n_R^{\max}} \right|, \quad (8)$$

where n_L^{\max} and n_R^{\max} are the peak values (i.e., maxima) of the total density pattern in the regions of $x \in (-\infty, 0)$ and $(0, \infty)$, respectively. If $\delta = 0$, the soliton has a symmetric density profile; otherwise, the soliton is asymmetric. Hence, the mechanism of the SSB can be characterized by a bifurcation diagram of δ by varying g or x_0 . The numerical simulations find that increasing the values of g or reducing the values of x_0 can lead to SSB of the soliton, which means that a stronger attractive nonlinearity and weaker coupling between the wells can easily lead to the SSB. The numerical results demonstrate that the current DWP can feature a similar property as in the usual DWPs, which is

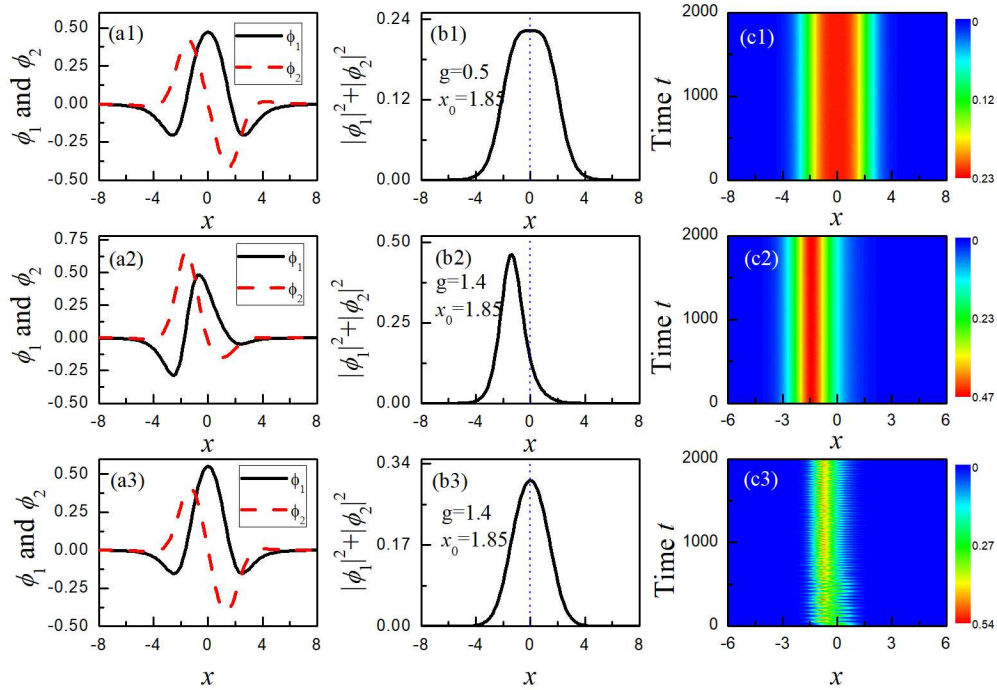


FIG. 3: (Color online) The profiles of the $\phi_1(x)$ and $\phi_2(x)$ components of the solutions are shown by the solid black and dashed red curves, respectively, for $g = 0.5, 1.4,$ and 1.4 , severally in panels (a1)-(a3). These example solutions correspond to the points a, b, and c marked in Fig. 2(a). The densities, i.e., $n(x)$, are shown in panels (b1)-(b3). The direct simulations of the perturbed evolution of $|\phi|^2$ are shown in panels (c1)-(c2). Here, the perturbation is 3% random noise, and the other parameters are $\gamma = 1, D = 2$ and $x_0 = 1.85$.

$\sim -\lambda(x)$. Two different kinds of SSB, displacement SSB and bimodal SSB, are found in this system by increasing g or reducing x_0 . The former type of SSB (i.e., displacement SSB) breaks the symmetry of single-peak solitons by shifting their center of mass from the origin of coordinates (i.e., $x = 0$), while the latter type of SSB (i.e., bimodal SSB) breaks the symmetry of a double-peak soliton by breaking the balance of the peak values. By increasing the values of g , displacement SSB tends to occur with a smaller value of x_0 , whereas bimodal SSB occurs with a larger value of x_0 . Figs. 2a and 2b show the bifurcation diagrams, which are displayed by δ versus g , for the displacement SSB and the bimodal SSB, respectively. The figures show that these two kinds of SSB are both supercritical, in which the asymmetric branches ($\delta \neq 0$) emerge as the stable branch ($\delta = 0$) and immediately go in the forward direction. Hence, these two types of SSB are tantamount to a phase transition of the second kind. Figs. 3 and 4 display typical examples of stable and unstable solitons for the two kinds of SSB, which are selected from the bifurcation diagrams in Figs. 2a and 2b (see the points ‘a’, ‘b’, and ‘c’ in these two panels).

In Figs. 3(a1), (a2) and (a3), one can see the amplitudes of the stable symmetric, asymmetric and unstable symmetric solitons, respectively, which correspond to points ‘a’, ‘b’, and ‘c’ in Fig. 2(a). These soliton solutions are complex functions that are specific to SO coupling (here, the imaginary parts is small). Their total density patterns, i.e., $n(x)$, which characterize their overall symmetry properties, are shown in Figs. 3(b1)-(b3). The direct simulations of the perturbed evolution of the soliton, which identify the stability and are shown by the evolution of the total density pattern, are displayed in panels 3(c1)-(c3). The reason why the phenomenon of displacement SSB tends to occur with smaller values x_0 can be explained as follows. The bottom of the DWP, i.e., $-\lambda(x)$, has a ‘W’ profile, which is constructed by a local maximum (at $x = 0$) and two adjacent minima (at $x = \pm x_0$). The difference between the center maximum and the two adjacent minima is denoted by the magnitude of x_0 . When x_0 is small, the difference is also small and is not enough to modulate the density pattern of the soliton. Hence, the soliton can maintain a single-peak profile and rest at the center when the nonlinearity is not obvious. However, if the nonlinearity is enhanced, the ground state is created in the adjacent minima; hence, the soliton shifts its center of mass away from the coordinate origin.

Fig. 4 shows a similar figure construction as in Fig. 3 for the case of bimodal SSB, which corresponds to points ‘a’, ‘b’, and ‘c’ in Fig. 2(b). The reason why the phenomenon of bimodal SSB tends to occur with a large value of x_0 can be explained by similar reasons as follows. When x_0 is large, the difference between the local maximum (at $x = 0$)

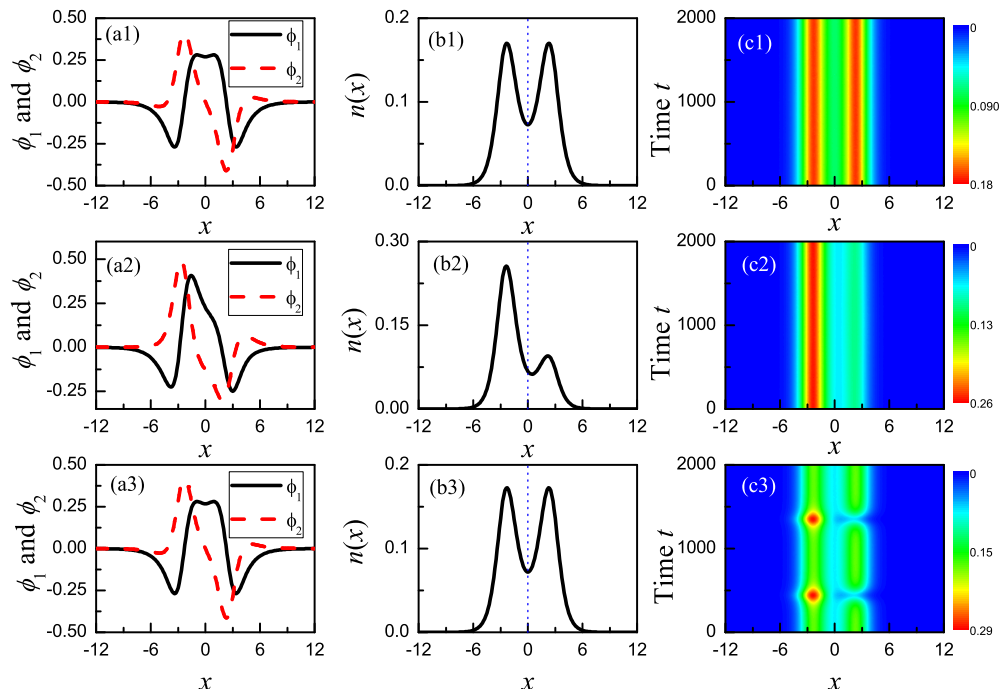


FIG. 4: (Color online) The profiles of the $\phi_1(x)$ and $\phi_2(x)$ components of the solutions are shown by the solid black and dashed red curves, respectively, for $g = 0.1, 0.25$, and 0.25 in panels (a1)-(a3). These example solutions correspond to the points a, b, and c marked in Fig. 2(b). The densities, i.e., $n(x)$, are shown in panels (b1)-(b3). The direct simulations of the perturbed evolution of $|\phi|^2$ are shown in panels (c1)-(c2). Here, the perturbation is 3% random noise, and the other parameters are $\gamma = 1$, $D = 2$ and $x_0 = 2.5$.

and the adjacent minima (at $x = \pm x_0$) becomes large. If this difference is large enough to modulate the density profile of the soliton, a soliton with a balanced double-peak structure is created when the nonlinearity is small. Then, if the nonlinearity is enhanced, SSB occurs and transforms the balanced double-peak structure into an imbalanced one.

The bifurcation point, g_{cr} as a function of x_0 for different values of γ , is displayed in Fig. 2c. A smaller value of g_{cr} implies that SSB is easier to induce. As expected, the figure shows that g_{cr} decreases as x_0 increases, which means that reducing the coupling between the two wells can easily induce SSB. The dividing points between displacement SSB and bimodal SSB are labeled in the curve of $g_{cr}(x_0)$ by the junction between the solid and the dash curves. The figure also shows that the magnitude of g_{cr} is also strongly influenced by the value of γ . Since the larger value of γ increases the effect of the total nonlinearity, the curve of $g_{cr}(x_0)$ with larger values of γ is lower than the curve with smaller values of γ . However, the figure shows that the dividing point between the two types of SSB does not show an obvious relationship with γ .

B. Moving reference frame

Unlike the usual DWP, the system in SO coupling does not obey Galilean invariance. Hence, the studies of SSB in a DWP formed by SO coupling is a nontrivial issue. Here, we assume the stable transfer of solitons by the moving SOC profile, which corresponds to Eq. (2) with

$$\lambda(x) \rightarrow \lambda(x'), \quad (9)$$

where $x' = x - ct$. The purpose of this subsection is to determine the influence of $c \neq 0$ on the SSB. For convenience, we will fix $\gamma = 1$ in this subsection.

To address this issue, Eq. (3) is rewritten in terms of the moving coordinate with the transformed wave function,

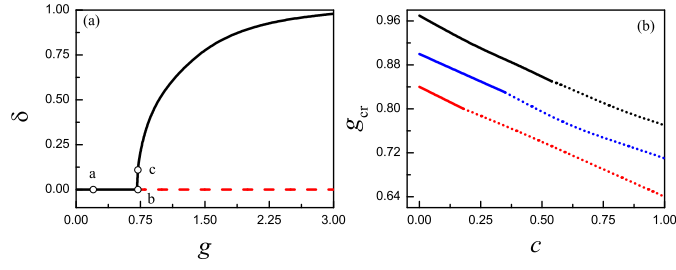


FIG. 5: (Color online) (a) Bifurcation diagrams for the symmetric and asymmetric solutions, in the plane of (g, δ) , as found from the numerical solution of Eq. (11) with $c = 1$. (b) The black, blue, and red curves show the displacement supercritical points for $x_0 = 1.825, 1.85,$ and 1.875 , respectively. The blue, black, and red dashed curves show the bimodal supercritical points for $x_0 = 1.825, 1.85,$ and 1.875 , respectively.

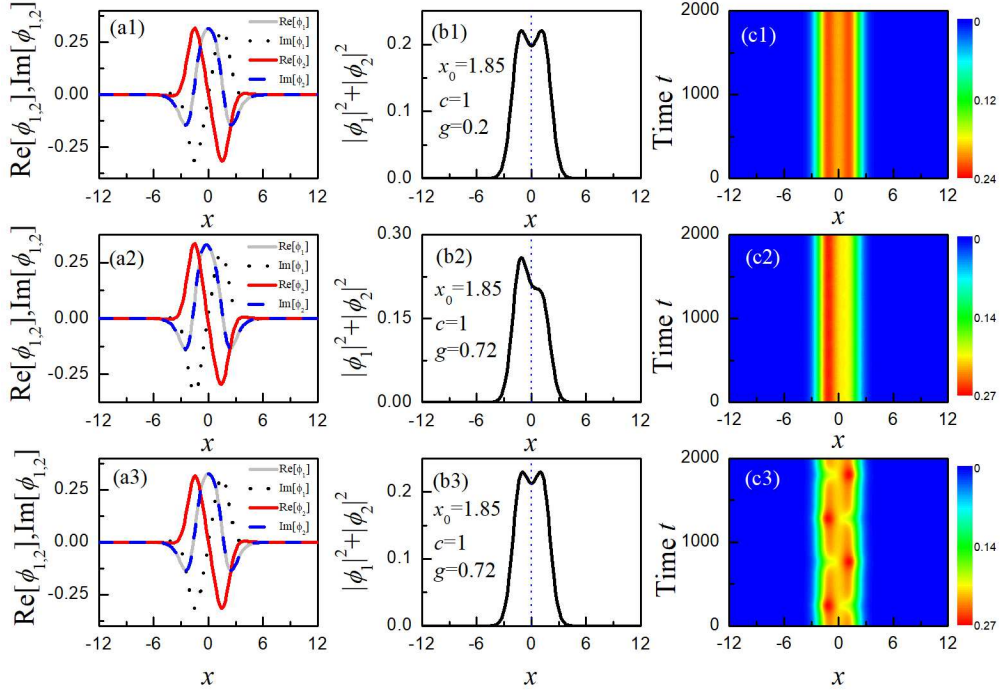


FIG. 6: (Color online) The real and imaginary parts of the $\phi_1(x)$ and $\phi_2(x)$ components of the solutions are shown by the solid gray, dotted black, solid red and dashed blue curves, respectively, for $g = 0.2, 0.72,$ and 0.72 in panels (a1)-(a3). These example solutions correspond to the points a, b, and c marked in Fig. 5(a). The densities, i.e., $n(x)$, are shown in panels (b1)-(b3). The direct simulations of the perturbed evolution of $|\phi|^2$ are shown in panels (c1)-(c2). Here, the perturbation is 3% random noise, and the other parameters are $\gamma = 1, D = 2, x_0 = 1.85$ and $c = 1$.

$\Psi_{\pm}(x, t) = \Psi_{\pm}(x', t)$, as

$$\begin{aligned}
 i \frac{\partial \Psi_+}{\partial t} &= -\frac{1}{2} \frac{\partial^2 \Psi_+}{\partial x'^2} + ic \frac{\partial \Psi_+}{\partial x'} - g \left(|\Psi_+|^2 + \gamma |\Psi_-|^2 \right) \Psi_+ + \lambda(x') \frac{\partial \Psi_-}{\partial x} + \frac{\lambda_{x'}(x')}{2} \Psi_-, \\
 i \frac{\partial \Psi_-}{\partial t} &= -\frac{1}{2} \frac{\partial^2 \Psi_-}{\partial x'^2} + ic \frac{\partial \Psi_-}{\partial x'} - g \left(|\Psi_-|^2 + \gamma |\Psi_+|^2 \right) \Psi_- - \lambda(x') \frac{\partial \Psi_+}{\partial x} - \frac{\lambda_{x'}(x')}{2} \Psi_+.
 \end{aligned} \tag{10}$$

Further, by applying the transformation

$$\Psi_{\pm}(x', t) = \Psi'_{\pm}(x', t) \exp[icx'^2/2],$$

Eq. (10) can be transformed to

$$\begin{aligned} i\frac{\partial\Psi'_+}{\partial t} &= -\frac{1}{2}\frac{\partial^2\Psi'_+}{\partial x'^2} - g\left(|\Psi'_+|^2 + \gamma|\Psi'_-|^2\right)\Psi'_+ + \lambda(x')\frac{\partial\Psi'_-}{\partial x'} + \frac{\lambda_{x'}(x')}{2}\Psi_- - ic\lambda(x')\Psi'_-, \\ i\frac{\partial\Psi'_-}{\partial t} &= -\frac{1}{2}\frac{\partial^2\Psi'_-}{\partial x'^2} - g\left(|\Psi'_-|^2 + \gamma|\Psi'_+|^2\right)\Psi'_- - \lambda(x')\frac{\partial\Psi'_+}{\partial x'} - \frac{\lambda_{x'}(x')}{2}\Psi'_+ + ic\lambda(x')\Psi'_+. \end{aligned} \quad (11)$$

In usual DWP systems, which are realized in homogeneous space, the transformation from Eq. (10) to (11) makes Eq. (11) have the same expression as Eq. (3), which is required for Galilean invariance. Hence, the variation in the magnitude of the velocity, c , will not influence the process of SSB. However, in the current system, Eq. (11) does not have the same expression as Eq. (3), and the magnitude of the velocity, c , will definitely influence the process of the SSB. It is necessary to mention that Galilean invariance can also be broken by applying a periodic boundary condition to the system. With a periodical boundary condition, the moving velocity changes to a rotational angular velocity. The SSB in the DWP system with a toroidal trap depends on the magnitude of the rotational velocity [88]. A recent study found that such a rotating system can emulate the SO coupling system [67], which reveals the internal connection between the rotating system and the effect of SO coupling.

The SSB of the soliton can be obtained by solving the stationary solutions to Eqs. (11). The definition of δ in Eq. (8) remains valid by replacing x' with x . A Numerical simulation shows that increasing the values of c can lead to SSB of the soliton. The reason the SSB is induced by c can be explained by Eq. (11). The last term in Eq. (11) creates a linear mixing between the two components. The linear mixing has the same profile of $\lambda(x')$, which enhances the difference between the local maximum (at $x' = 0$) and the two adjacent minima (at $x' = \pm x_0$). The value of c is the strength of such linear mixing. Hence, increasing the value of c may reduce the coupling between the two wells, which makes the SSB easier to induce.

By selecting different values of x_0 , displacement SSB and bimodal SSB can be found and adjusted by the parameter c . Fig. 5a shows a typical example of the bifurcation map of the bimodal SSB induced by c . Typical examples of the symmetric and asymmetric solitons, which are labeled by 'a', 'b', and 'c' in Fig. 5a, are displayed in Fig. 6. It is interesting to note that the evolution of the unstable symmetric solution, which is shown in Fig. 6(c3), shows a typical Josephson Oscillation [89]. Josephson Oscillation in a DWP with homogeneous SO coupling and a moving system were report in Refs. [90, 91], respectively. This result implies that the current system may have potential in matter-wave interferometry [92, 93].

Fig. 5b displays g_{cr} as a function of c with different values of x_0 . The figure shows that an increase in c causes a transition between displacement SSB and bimodal SSB. The dividing point between displacement SSB and bimodal SSB can be adjusted by the values of x_0 and c .

IV. CONCLUSION

The objective of this work was to study the SSB of a soliton created in spinor BECs with spatially confined SO coupling formed by a two-spot laser beam. Two types of SSB, displacement symmetry breaking and bimodal symmetry breaking, are found in the system. Both types are supercritical, which indicates that these two kinds of SSB are tantamount to a phase transition of the second kind. By increasing the strength of the nonlinearity, displacement SSB tends to occur when the two spots of the SO coupling are close enough; however, when the distance between the two spots becomes large, bimodal SSB will occur, taking the place of displacement SSB. The explanation for the transition between these two kinds of SSB is discussed in detail in this paper. SSB in the moving reference is also considered because the SO coupling system in the moving reference frame is a nontrivial issue. The results show that the velocity plays an important role in influencing the SSB. Increasing the velocity may not only help to induce the SSB but also help the transition from displacement SSB to bimodal SSB.

A natural continuation of the current work is to consider this problem in 2D, assuming the BECs are trapped in a 2D plane and illuminated by two SO coupling spots. Hence, the inclusion of 2D vortices may generate more degrees of freedoms to influence the SSB. A more challenging option is to consider the current setup in a full 3D geometry.

Acknowledgments

This work was supported by NNSFC (China) through grants No. 11874112, 11575063, Foundation for Distinguished Young Talents in Higher Education of Guangdong No. 2018KQNCX279, 2018KQNCX009, and the Special Funds for the Cultivation of Guangdong College Students Scientific and Technological Innovation No. pdjh2019b0514.

Conflict of interest The authors declare that there is no conflict of interest to report.

-
- [1] Meystre, P.: *Atom Optics*, Springer. Berlin, 2002.
- [2] Burger, S., Bongs, K., Dettmer, S., Ertmer, W., Sengstock, K., Sanpera, A., Shlyapnikov, G. V., and Lewenstein, M.: Dark Solitons in Bose-Einstein Condensates. *Phys. Rev. Lett.* **83**, 5198 (1999).
- [3] Denschlag, J., Simsarian, J. E., Feder, D. L., Clark, C. W., Collins, L. A., Cubizolles, J., Deng, L., Hagley, E. W., Helmerson, K., Reinhardt, W. P., Rolston, S. L., Schneider, B. I., and Phillips, W. D.: Generating solitons by phase engineering of a Bose-Einstein condensate. *Science* **287**, 97 (2000).
- [4] Khaykovich, L., Schreck, F., Ferrari, G., Bourdel, T., Cubizolles, J., Carr, L. D., Castin, Y., and Salomon, C.: Formation of a Matter-Wave Bright Soliton. *Science* **296**, 1290 (2002).
- [5] Strecker, K. E., Partridge, G. B., Truscott, A. G., and Hulet, R. G.: Formation and propagation of matter-wave soliton trains. *Nature (London)* **417**, 150 (2002).
- [6] Mežnaršič, T., Arh, T., Brenc, J., Pišljar, J., Gosar, K., Gosar, Ž., Žitko, R., Zupanič, E., and Jeglič, P.: Cesium bright matter-wave solitons and soliton trains. *Phys. Rev. A* **99**, 033625 (2019).
- [7] Pal, R., Loomba, S., Kumar, C. N., Milovic, D., Maluckov, A.: Matter wave soliton solutions for driven Gross-Pitaevskii equation with distributed coefficients. *Annals of Physics* **401**, 116 (2019).
- [8] Kengne, E., and Liu, W. M.: Management of matter-wave solitons in Bose-Einstein condensates with time-dependent atomic scattering length in a time-dependent parabolic complex potential. *Phys. Rev. E* **98**, 012224 (2018).
- [9] Malomed, B. A.: Creating solitons by means of spin-orbit coupling. *EPL*, **122**, 36001 (2018).
- [10] Chen, G. P., Zhang, Z. Y., Dong, B., Wang, L. X., Zhang, X. F., Zhang, S. G.: Ground-state and rotational properties of a two-component Bose-Einstein condensate in a harmonic plus quartic trap. *Physics Letters A* **379**, 2193 (2015).
- [11] McDonald, G. D., Kuhn, C. C. N., Hardman, K. S., Bennetts, S., Everitt, P. J., Altin, P. A., Debs, J. E., Close, J. D., and Robins, N. P.: Bright Solitonic Matter-Wave Interferometer. *Phys. Rev. Lett.* **113**, 013002 (2014).
- [12] Schmitt, M., Wenzel, M., Böttcher, F., Ferrier-Barbut, I., and Pfau, T.: Self-bound droplets of a dilute magnetic quantum liquid. *Nature* **539**, 259 (2016).
- [13] Chomaz, L., Baier, S., Petter, D., Mark, M. J., Wächtler, F., Santos, L., and Ferlaino, F.: Quantum-fluctuation-driven crossover from a dilute Bose-Einstein condensate to a macrodroplet in a dipolar quantum fluid. *Phys. Rev. X* **6**, 041039 (2016).
- [14] Cabrera, C. R., Tanzi, L., Sanz, J., Naylor, B., Thomas, P., Cheiney, P., Tarruell, L.: Quantum liquid droplets in a mixture of Bose-Einstein condensates. *Science* **359**, 301 (2018).
- [15] Petrov, D. S.: Quantum mechanical stabilization of a collapsing Bose-Bose mixture. *Phys. Rev. Lett.* **115**, 155302 (2015).
- [16] Wächtler, F., and Santos, L.: Ground-state properties and elementary excitations of quantum droplets in dipolar Bose-Einstein condensates. *Phys. Rev. A* **94**, 043618 (2016).
- [17] Baillie, D., Wilson, R. M., Bisset, R. N., and Blakie, P. B.: Self-bound dipolar droplet: A localized matter wave in free space. *Phys. Rev. A* **94**, 021602(R) (2016).
- [18] Edler, D., Mishra, C., Wächtler, F., Nath, R., Sinha, S., and Santos, L.: Quantum Fluctuations in Quasi-One-Dimensional Dipolar Bose-Einstein Condensates. *Phys. Rev. Lett.* **119**, 050403 (2017).
- [19] Ferrier-Barbut, I., Kadau, H., Schmitt, M., Wenzel, M., and Pfau, T.: Observation of Quantum Droplets in a Strongly Dipolar Bose Gas. *Phys. Rev. Lett.* **116**, 215301 (2016).
- [20] Cidrim, A., dos Santos, F. E. A., Henn, E. A. L., and Macrì, T.: Vortices in self-bound dipolar droplets. *Phys. Rev. A* **98**, 023618 (2018).
- [21] Bisset, R. N., Wilson, R. M., Baillie, D., and Blakie, P. B.: Ground-state phase diagram of a dipolar condensate with quantum fluctuations. *Phys. Rev. A* **94**, 033619 (2016).
- [22] Sekino, Y., and Nishida, Y.: Quantum droplet of one-dimensional bosons with a three-body attraction. *Phys. Rev. A* **97**, 011602(R) (2018).
- [23] Li, Y., Luo, Z., Liu, Y., Chen, Z., Huang, C., Fu, S., Tan, H., and Malomed, B. A.: Two-dimensional solitons and quantum droplets supported by competing self- and cross-interactions in spin-orbit-coupled condensates. *New J. Phys.* **19**, 113043 (2017).
- [24] Li, Y., Chen, Z., Luo, Z., Huang, C., Tan, H., Pang, W., and Malomed, B. A.: Two-dimensional vortex quantum droplets. *Phys. Rev. A* **98**, 063602 (2018).
- [25] Kartashov, Y. V., Malomed, B. A., and Torner, L.: Metastability of Quantum Droplet Clusters. *Phys. Rev. Lett.* **122**, 193902 (2019).
- [26] Ferioli, G., Semeghini, G., Masi, L., Giusti, G., Modugno, G., Inguscio, M., Gallem, A., Recati, A., and Fattori, M.: Collisions of Self-Bound Quantum Droplets. *Phys. Rev. Lett.* **122**, 090401 (2019).
- [27] Staudinger, C., Mazzanti, F., and Zillich, R. E.: Self-bound Bose mixtures. *Phys. Rev. A* **98**, 023633 (2018).
- [28] Cikojević, V., Dželalija, K., Stipanović, P., and Markić, L. V.: Ultradilute quantum liquid droplets. *Phys. Rev. B* **97**, 140502 (R) (2018).
- [29] Astrakharchik, G. E., and Malomed, B. A.: Dynamics of one-dimensional quantum droplets. *Phys. Rev. A* **98**, 013631 (2018).
- [30] Semeghini, G., Ferioli, G., Masi, L., Mazzi, C., Wolszki, L., Minardi, F., Modugno, M., Modugno, G., Inguscio, M.,

- and Fattori, M.: Self-bound quantum droplets in atomic mixtures. *Phys. Rev. Lett.* **120**, 235301 (2018).
- [31] Cappellaro, A., Macrì, T., and Salasnich, L.: Collective modes across the soliton-droplet crossover in binary Bose mixtures. *Phys. Rev. A* **97**, 053623 (2018).
- [32] Cui, X.: Spin-orbit-coupling-induced quantum droplet in ultracold Bose-Fermi mixtures. *Phys. Rev. A* **98**, 023630 (2018).
- [33] Liu, B., Zhang, H., Zhong, R., Zhang, X., Qin, X., Huang, Ch., Li, Y., and Malomed, B. A.: Symmetry breaking of quantum droplets in a dual-core trap. *Phys. Rev. A* **99**, 053602 (2019).
- [34] Westerberg, N., Wilson, K. E., Duncan, C. W., Faccio, D., Wright, E. M., Öhberg, P., and Valiente, M.: Self-bound droplets of light with orbital angular momentum. *Phys. Rev. A* **98**, 053835 (2018).
- [35] Zhang, R. F., Zhang, X. F., Li, L.: Exotic vortex structures of the dipolar Bose-Einstein condensates trapped in harmonic-like and toroidal potential. *Physics Letters A* **383**, 231 (2019).
- [36] Pedri, P., and Santos, L.: Two-Dimensional Bright Solitons in Dipolar Bose-Einstein Condensates. *Phys. Rev. Lett.* **95**, 200404 (2005).
- [37] Tikhonenkov, I., Malomed, B. A., and Vardi, A.: Anisotropic Solitons in Dipolar Bose-Einstein Condensates. *Phys. Rev. Lett.* **100**, 090406 (2008).
- [38] Tikhonenkov, I., Malomed, B. A., and Vardi, A.: Vortex solitons in dipolar Bose-Einstein condensates. *Phys. Rev. A* **78**, 043614 (2008).
- [39] Chen, X., Chuang, Y., Lin, C., Wu, C., Li, Y., Malomed, B. A., and Lee, R.: Magic tilt angle for stabilizing two-dimensional solitons by dipole-dipole interactions. *Phys. Rev. A* **96**, 043631 (2017).
- [40] Xu, Y., Zhang, Y., and Wu, B.: Bright solitons in spin-orbit coupled Bose-Einstein condensates. *Phys. Rev. A* **87**, 013614 (2013).
- [41] Sakaguchi, H., Li, B., Malomed, B. A.: Creation of two-dimensional composite solitons in spin-orbit-coupled self-attractive bose-einstein condensates in free space. *Phys Rev E* **89**, 032920 (2014).
- [42] Zhang, Y., Zhou, Zh., Malomed, B. A., and Pu, H.: Stable solitons in three dimensional free space without the ground state: self-trapped bose-einstein condensates with spin-orbit coupling. *Phys Rev Lett* **115**, 253902 (2015).
- [43] Zhai, H.: Degenerate quantum gases with spin-orbit coupling: a review. *Rep. Prog. Phys.* **78**, 026001 (2015).
- [44] Chen, G., Liu, Y., Huang, H.: Mixed-mode solitons in quadrupolar BECs with spin-orbit coupling. *Commun. Nonlinear. Sci. Numer. Simulat.* **48**, 318 (2017).
- [45] Zhang, Y., Mossman, M. E., Busch, T., Engels, P., Zhang, C.: Properties of spin-orbit-coupled Bose-Einstein condensates. *Front. Phys.* **11**, 118103 (2016).
- [46] Wen, L., Liang, Y., Zhou, J., Yu, P., Xia, L., Niu, L., Zhang, X.: Effects of linear Zeeman splitting on the dynamics of bright solitons in spin-orbit coupled Bose-Einstein condensates. *Acta Physica Sinica* **68**, 080301 (2019).
- [47] Wen, L., Sun, Q., Wang, H. Q., Ji, A. C., and Liu, W. M.: Ground state of spin-1 Bose-Einstein condensates with spin-orbit coupling in a Zeeman field. *Phys. Rev. A* **86**, 043602 (2012).
- [48] Wang, L., Dai, C., Wen, L., Liu, T., Jiang, H., Saito, H., Zhang, S., and Zhang, X.: Dynamics of vortices followed by the collapse of ring dark solitons in a two-component Bose-Einstein condensate. *Phys. Rev. A* **97**, 063607 (2018).
- [49] Li, Y., Liu, Y., Fan, Z., Pang, W., Fu, S., and Malomed, B. A.: Two dimensional dipolar gap solitons in free space with spin-orbit coupling. *Phys. Rev. A* **95**, 063613 (2017).
- [50] Xu, T. F., Li, W. L., Li, Z. D., Zhang, C.: Phase diagram and dynamics of dark-bright vector solitons in spin-orbit-coupled Bose-Einstein condensate. *Chaos, Solitons and Fractals* **111**, 62 (2018).
- [51] Sabari, S., Porsezian, K., Muruganandam, P.: Dynamical stabilization of two-dimensional trapless Bose-Einstein condensates by three-body interaction and quantum fluctuations. *Chaos, Solitons and Fractals* **103**, 232 (2018).
- [52] Zhong, R., Chen, Z., Huang, C., Luo, Z., Tan, H., Malomed, B. A., Li, Y.: Self-trapping under two-dimensional spin-orbit coupling and spatially growing repulsive nonlinearity. *Front. of Physics*, **13**, 130311 (2018).
- [53] Sakaguchi, H.: New models for multi-dimensional stable vortex solitons. *Frontiers of Physics*, **14**, 12301 (2018).
- [54] Huang, C., Ye, Y., Liu, S., He, H., Pang, W., Malomed, B. A., and Li, Y.: Excited states of two-dimensional solitons supported by spin-orbit coupling and field-induced dipole-dipole repulsion. *Phys. Rev. A* **97**, 013636 (2018).
- [55] Kartashov, Y. V., Konotop, V. V., and Abdullaev, F. Kh.: Gap Solitons in a Spin-Orbit-Coupled Bose-Einstein Condensate. *Phys. Rev. Lett.* **111**, 060402 (2013).
- [56] Sakaguchi, H., Malomed, B. A.: One- and two-dimensional gap solitons in spin-orbit-coupled systems with Zeeman splitting. *Phys. Rev. A* **97**, 013607 (2018).
- [57] Sakaguchi, H., Sherman, E. Y., Malomed, B. A.: Vortex solitons in two-dimensional spin-orbit coupled Bose-Einstein condensates: Effects of the Rashba-Dresselhaus coupling and Zeeman splitting. *Phys. Rev. E* **94**, 032202 (2016).
- [58] Gautam, S., and Adhikari, S. K.: Vortex-bright solitons in a spin-orbit-coupled spin-1 condensate. *Phys. Rev. A* **95**, 013608 (2017).
- [59] Jiang, X., Fan, Z., Chen, Z., Pang, W., Li, Y., and Malomed, B. A.: Two-dimensional solitons in dipolar Bose-Einstein condensates with spin-orbit coupling. *Phys. Rev. A* **93**, 023633 (2016).
- [60] Liao, B., Liu, S., Huang, C., Luo, Z., Pang, W., Tan, H., Malomed, B. A., and Li, Y.: Anisotropic semivortices in dipolar spinor condensates controlled by Zeeman splitting. *Phys. Rev. A* **96**, 043613 (2017).
- [61] Liao, B., Ye, Y., Zhuang, J., Huang, C., Deng, H., Pang, W., Liu, B., Li, Y.: Anisotropic solitary semivortices in dipolar spinor condensates controlled by the two-dimensional anisotropic spin-orbit coupling. *Chaos, Solitons and Fractals*, **116**, 424 (2018).
- [62] Liu, S., Liao, B., Kong, J., Chen, P., Lü, J., Li, Y., Huang, C., and Li, Y.: Anisotropic Semi Vortices in Spinor Dipolar Bose Einstein Condensates Induced by Mixture of Rashba Dresselhaus Coupling. *J. Phys. Soc. Jpn.* **87**, 094005 (2018).

- [63] Pang, W., Deng, H., Liu, B., Xu, J., and Li, Y.: Two-Dimensional Vortex Solitons in Spin-Orbit-Coupled Dipolar Bose-Einstein Condensates. *Applied Science*, **8**, 1771(2018).
- [64] Wen, L., Zhang, X., Hu, A., Zhou, J., Yu, P., Xia, L., Sun, Q., Ji, A.-C.: Dynamics of bright-bright solitons in Bose-Einstein condensate with Raman-induced one-dimensional spin-orbit coupling. *Annals of Physics* **390**, 180 (2018).
- [65] Kartashov, Y. V., Malomed, B. A., Konotop, V. V., Lobanov, V. E., and Torner, L.: Stabilization of spatiotemporal solitons in Kerr media by dispersive coupling. *Opt. Lett.* **40**, 1045 (2015).
- [66] Sakaguchi, H., Malomed, B. A.: One- and two-dimensional solitons in symmetric systems emulating spin-orbit coupling. *New J. Phys.* **18** 105005 (2016).
- [67] Huang, H., Lyu, L., Xie, M., Luo, W., Chen, Z., Luo, Z., Huang, C., Fu, S., Li, Y.: Spatiotemporal solitary modes in a twisted cylinder waveguide shell with the self-focusing Kerr nonlinearity. *Commun. Nonlinear Sci. Numer. Simulat.* **67**, 617(2019).
- [68] Dai, C., Zhou, G., Chen, R., Lai, X., Zheng, J.: Vector multipole and vortex solitons in two-dimensional Kerr media. *Nonlinear Dyn.* **88**, 2629 (2017).
- [69] Dai, C., Chen, R., Wang, Y., Fan, Y.: Dynamics of light bullets in inhomogeneous cubic-quintic-septimal nonlinear media with PT-symmetric potentials. *Nonlinear Dyn.* **87**, 1675 (2017).
- [70] Kartashov, Y., Konotop, V., Zezyulin, D.: Bose-einstein condensates with localized spin-orbit coupling: soliton complexes and spinor dynamics. *Phys Rev A* **90**, 063621 (2014).
- [71] Li, Y., Zhang, X., Zhong, R., Luo, Z., Liu, B., Huang, C., Pang, W., Malomed, B. A.: Two-dimensional composite solitons in Bose-Einstein condensates with spatially confined spin-orbit coupling. *Commun Nonlinear Sci Numer Simulat* **73**, 481 (2019).
- [72] Eilbeck, J. C., Lomdahl, P. S., and Scott, A. C.: The discrete self-trapping equation. *Physica D* **16**, 318 (1985).
- [73] Yannouleas, C., Landman, U.: Group theoretical analysis of symmetry breaking in two dimensional quantum dots. *Phys. Rev. B* **68**, 035325 (2003).
- [74] Herring, G., Kevrekidis, P. G., Malomed, B. A., Carretero-González, R., Frantzeskakis, D. J.: Symmetry breaking in linearly coupled dynamical lattices. *Phys. Rev. E* **76**, 066606 (2007).
- [75] Hung, N. V., Trippenbach, M., Malomed, B. A.: Symmetric and asymmetric solitons trapped in H-shaped potentials. *Phys. Rev. A* **84**, 053618 (2011).
- [76] Esry, B. D., Greene, C. H.: Spontaneous spatial symmetry breaking in two-component Bose-Einstein condensates. *Phys. Rev. A* **59**, 1457 (1999).
- [77] Wu, B., Niu, Q.: Landau and dynamical instabilities of the superflow of Bose-Einstein condensates in optical lattices. *Phys. Rev. A* **64**, 061603 (2001).
- [78] Sadler, L. E., Higbie, J. M., Leslie, S. R., Vengalattore, M., Stamper-Kurn, D. M.: Spontaneous symmetry breaking in a quenched ferromagnetic spinor Bose-Einstein condensate. *Nature* **443**, 312 (2006).
- [79] Xiong, B., Gong, J. B., Pu, H., Bao, W. Z., Li, B. W.: Symmetry breaking and self-trapping of a dipolar Bose-Einstein condensate in a double-well potential. *Phys. Rev. A* **79**, 013626 (2009).
- [80] Adhikari, S. K., Malomed, B. A., Salasnich, L., Toigo, F.: Spontaneous symmetry breaking of Bose-Fermi mixtures in double-well potentials. *Phys. Rev. A* **81**, 053630 (2010).
- [81] Li, Y., Fan, Z., Luo, Z., Liu, Y., He, H., Lü, J., Xie, J., Huang, C., Tan, H.: Cross-symmetry breaking of two-component discrete dipolar matter-wave solitons. *Front. Phys.* **12**, 124206 (2017).
- [82] Li, Y., Pang, W., and Malomed, B. A.: Nonlinear modes and symmetry breaking in rotating double-well potentials. *Phys. Rev. A* **86**, 023832 (2012).
- [83] Li, Y., Liu, J., Pang, W., and Malomed, B. A.: Symmetry breaking in dipolar matter-wave solitons in dual-core couplers. *Phys. Rev. A* **87**, 013604 (2013).
- [84] Zhu, Q. Z., Zhang, Q., and Wu, B.: Extended two-site Bose-Hubbard model with pair tunneling: spontaneous symmetry breaking, effective ground state and fragmentation. *J. Phys. B: At. Mol. Opt. Phys.* **48**, 045301 (2015).
- [85] Malomed, B. A.: Spontaneous symmetry breaking in nonlinear systems: An overview and a simple model, in *Nonlinear Dynamics: Materials, Theory and Experiments*, edited by M. Tlidi and M. G. Clerc (Springer, Heidelberg, 2016).
- [86] Chiofalo, L. M., Succi, S., and Tosi, P. M.: Ground state of trapped interacting Bose-Einstein condensates by an explicit imaginary time algorithm. *Phys. Rev. E* **62**, 7438 (2000).
- [87] Yang, J., and Lakoba, T. I.: Accelerated imaginary-time evolution methods for the computation of solitary waves. *Stud. Appl. Math.* **120**, 265 (2008).
- [88] Chen, G., Wang, H., Chen, Z., Liu, Y.: Fundamental modes in waveguide pipe twisted by saturated double-well potential. *Frontiers of Physics* **12**, 124201 (2017).
- [89] Albiez, M., Gati, R., Fölling, J., Hunsmann, S., Cristiani, M., and Oberthaler, M. K.: Direct Observation of Tunneling and Nonlinear Self-Trapping in a Single Bosonic Josephson Junction. *Phys. Rev. Lett.* **95**, 010402 (2005).
- [90] Zhang, D., Fu, L., Wang, Z., and Zhu, S.: Josephson dynamics of a spin-orbit-coupled Bose-Einstein condensate in a double-well potential. *Phys. Rev. A* **85**, 043609 (2012).
- [91] Guo, H., Chen, Z., Liu, J., and Li, Y.: Fundamental modes in a waveguide pipe twisted by inverted nonlinear double-well potential. *Laser Phys.* **24**, 045403 (2014).
- [92] Shin, Y., Saba, M., Pasquini, T. A., Ketterle, W., Pritchard, D. E., and Leanhardt, A. E.: Stable Solitons in Three Dimensional Free Space without the Ground State: Self-Trapped Bose-Einstein Condensates with Spin-Orbit Coupling. *Phys. Rev. Lett.* **92**, 050405(2004).
- [93] Schumm, T., Hofferberth, S., Andersson, L. M., Wildermuth, S., Groth, S., Bar-Joseph, I., Schmiedmayer, J., and Krüger, P.: Matter-wave interferometry in a double well on an atom chip. *Nat. Phys.* **1**, 57 (2005).